

# Drug diffusion in hydrophobically modified *N,N*-dimethylacrylamide hydrogels

Matthew P. Mullarney<sup>a,1</sup>, Thomas A.P. Seery<sup>b,c,2</sup>, R.A. Weiss<sup>a,b,\*</sup>

<sup>a</sup> Chemical Engineering Department, University of Connecticut, Storrs, CT 06269, USA

<sup>b</sup> Polymer Program, Institute of Materials Science, University of Connecticut, Storrs, CT 06269, USA

<sup>c</sup> Chemistry Department, University of Connecticut, Storrs, CT 06269, USA

Received 5 February 2006; received in revised form 22 March 2006; accepted 23 March 2006

## Abstract

The use of hydrophobically modified hydrogels for drug release was investigated. Copolymers of *N,N*-dimethylacrylamide and 2-(*N*-ethyl-perfluorooctanesulfonamido) ethyl acrylate (FOSA) were prepared by free-radical polymerization. The drug release rates, dynamic swelling behavior, and pH sensitivities of copolymers ranging in composition from 0 to 30 mol% FOSA were studied. Pheniramine maleate, an ocular antihistamine, was used as the model drug substance. Hydrogels of DMA produced with increasing amounts of FOSA had a decreased equilibrium media content and exhibited a slower drug release rate. Early-time, late-time and Etters approximation drug diffusion coefficients ranged from  $0.4 \times 10^{-3}$  to  $12.3 \times 10^{-3}$  mm<sup>2</sup>/min. The diffusion of the drug model was less sensitive to pH of the buffered media over the range of pH 4–8, but increasing the media pH slowed the permeability slightly by decreasing the swellability of the hydrogel. The power law exponent ( $n \approx 0.5$ ) and the swelling interface number ( $Sw \gg 1$ ) suggested that the drug release mechanism from these hydrogels was Fickian and not swelling controlled. These novel thermoprocessible hydrogels have potential to be used as controlled ocular drug delivery devices (e.g. contact lenses or ocular inserts).

© 2006 Elsevier Ltd. All rights reserved.

**Keywords:** Hydrogel; Dimethylacrylamide; Pheniramine

## 1. Introduction

A hydrogel is a network of polymer chains that absorbs and retains a significant amount of water (>20%). The water content in the hydrogels depends on the hydrophilicity of the chains and degree of crosslinking in the network [1]. The behavior of water within the hydrogel is important to understand because it dominates the physical and transport properties of the hydrogel. It has been reported that hydrogels contain three ‘types’ of water: free water, intermediate water, and bound water [2]. Free water can move through the network without significant attractive or repulsive interactions with

the polymeric network. Bound water is joined to the polymer through hydrogen bonds, and intermediate water is thought to exchange with the bound and free water. When polymers are highly hydrophilic they typically contain a greater proportion of bound water; therefore, the hydrophilicity of the polymer can significantly affect the swelling and transport behavior of the hydrogel.

In their dehydrated state, hydrogels are not very different from common polymers. However, hydrated hydrogels are unique, because they can have the structural integrity of a solid and still exhibit the diffusive transport properties of a liquid [3]. These attributes make hydrogels attractive for use as biomedical devices, e.g. transdermal patches and implants. They can be either chemically crosslinked with irreversible bonds or physically crosslinked with reversible bonds depending on the monomers, polymerization method, and the application [4]. Recent research has focused on synthesizing and characterizing hydrogels that exhibit particular mechanical properties such as strength and modulus, environmental responsiveness to temperature, electric field, pH or ionic strength, and mass transport control that can be ‘tuned’ to achieve very specific pharmacological applications. For

\* Corresponding author. Address: Polymer Program, Institute of Materials Science, University of Connecticut, 97 N. Eagleville Rd., Storrs, CT 06269, USA. Tel.: +1 860 486 4698.

E-mail addresses: [matthew\\_p\\_mullarney@groton.pfizer.com](mailto:matthew_p_mullarney@groton.pfizer.com) (M.P. Mullarney), [seery@mail.ims.uconn.edu](mailto:seery@mail.ims.uconn.edu) (T.A.P. Seery), [rweiss@mail.ims.uconn.edu](mailto:rweiss@mail.ims.uconn.edu) (R.A. Weiss).

<sup>1</sup> Tel.: +1 860 715 4139.

<sup>2</sup> Tel.: +1 860 486 1337.

example, a well constructed hydrogel can help to reduce toxic ‘burst’ effects of a drug, protect fragile drugs in their dosing environment and allow location-specific dosing [5]. Hydrogels comprised of monomers such as 2-hydroxyethyl methacrylate (HEMA), *N*-vinyl pyrrolidone (NVP), vinyl alcohol (VA), ethylene oxide (EO), ethylene glycol (EG), and methyl methacrylate (MMA) have been generally well studied [1], but research continues to improve and optimize hydrogel properties.

One particular monomer that has received much attention is *N,N*-dimethylacrylamide (DMA), which can be polymerized into a highly hydrophilic and biocompatible hydrogel. However, even when chemically crosslinked, poly(DMA) exhibits rather low mechanical strength. To overcome this deficiency, DMA can be copolymerized with a hydrophobic monomer, and the glass transition temperature and water sorption and desorption kinetics of the hydrogel can be modified by changing the structure, location, or concentration of the hydrophobic group [6]. Therefore, hydrophobically modified hydrogels are of significant interest because their properties can be ‘tuned’. Related studies have shown that 5–30 wt% of the hydrophobic monomer MMA can be copolymerized with DMA to achieve an optimal balance between mechanical strength and water content [7]. Equilibrium water contents from 70 to 97% and Young’s modulus from  $\sim 0$  to 0.5 MPa were achievable by varying the MMA concentration. DMS has been used for contact lenses [8–10], because of its optical transparency, low modulus of elasticity and high oxygen permeability. Unfortunately, those hydrogels phase-separate, where poly(DMS) separates from the hydrophilic phase and polar solvents. That obstacle can be overcome by using fluorinated side chain siloxanes with terminal  $-\text{CF}_2-\text{H}$  in copolymers of *N*-vinyl pyrrolidone and DMA. Such transparent hydrogels demonstrated low modulus while maintaining high water content and oxygen permeability. Therefore, the use of comonomers containing perfluoro side chains with DMA has proved promising for improving poly(DMA) properties.

Hogen-Esch and co-workers [11–15] demonstrated that the introduction of physical crosslinks from a hydrophobic fluorocarbon monomer such as 2-(*N*-ethyl-perfluorooctanesulfonamido) ethyl acrylate (FOSA) can modify the rheological and physical properties of acrylamide copolymers and conceivably control drug diffusion. That is an exciting prospect

because these copolymers are thermally processable [8], which is attractive for exploiting manufacturing processes such as extrusion and injection molding, and this would enable a mechanically robust DMA-based hydrogel to be used as an effective drug delivery system. Similar hydrophilic/hydrophobic systems for controlling the diffusion of both large and small drug molecules and adjust these systems to exhibit zero-order, first-order, or bimodal release are reported in the literature [16–19].

Although DMA copolymers with significant concentrations of FOSA have been studied and characterized [8,20–22], the effects of FOSA on drug diffusion have not been specifically investigated. If FOSA can be used to improve or modify the properties of DMA-based hydrogels, these materials could have a significant potential for drug delivery applications based on contact lenses or ocular inserts. In order for these materials to be seriously considered for use in vivo, they must exhibit stable behavior in environments of different pH. The objective of the present work was to determine the effect of the hydrophobic comonomer, FOSA, on controlling the drug diffusion rate and/or drug diffusion mechanism in DMA-based hydrogels.

## 2. Experimental

### 2.1. Materials and polymer preparation

The two monomers *N,N*-dimethylacrylamide (DMA) (Sigma–Aldrich, St. Louis, MO) and 2-(*N*-ethyl-perfluorooctanesulfonamido) ethyl acrylate (FOSA) (3 M, St Paul, MN) were used to prepare the polymers for this study. The structures of these monomers are shown in Fig. 1. Copolymers of DMA and FOSA were prepared according to previously reported methods by free-radical polymerization using 2,2’-azo-bisobutyronitrile as the initiator and 1,4-dioxane as the solvent [6]. Previous work showed that hydrophobic associations of the FOSA units produced a physically crosslinked structure. For comparison to the copolymers, a chemically crosslinked homopolymer of poly(DMA) was also prepared according to previously reported methods [21] by redox polymerization using *N,N*’-methylene bisacrylamide as the crosslinker, *N,N,N,N*’-tetramethylethylenediamine as the initiator, ammonium persulfate as the accelerator, and water as the solvent. The copolymer compositions, which ranged from 0 to

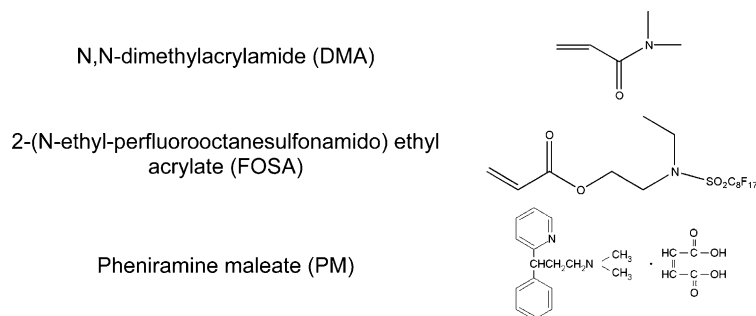


Fig. 1. Structure of monomers (DMA and FOSA) and drug substance (PM).

Table 1  
Composition of FOSA–DMA copolymers (50 g batch)

Sample	FOSA (mol%)	FOSA (wt%)	FOSA (g)	DMA (g)	AIBN (mg)	$T_g^a$ (°C)
DF0	0	0	0	50	–	124
DF5	5.4	26	13.5	36.5	65	111
DF10	9.8	41	19.4	30.6	55	99
DF20	20.4	62	28.4	20.6	40	91
DF29	28.9	72	37.5	12.5	30	80

<sup>a</sup> Ref. [22].

30 mol% FOSA, are summarized in Table 1. The nomenclature used herein for the copolymers is DFXX-Y, where XX represents the mol% FOSA in the polymer and Y represents the buffered media pH.

For the diffusion studies, the dry copolymers were compression molded into ~1 mm thick films with a hydraulic heat press at ~50 °C above its glass transition temperature ( $T_g$ ). The DMA homopolymer was cast into a ~1 mm thick film during polymerization. The polymer films were washed in deionized water for 7 days to remove any residual monomers, initiator, and crosslinking agent. Disks were cut from the wet films using a custom-made cork borer (18 mm diameter) and then vacuum dried over desiccant for 1 week at 21 °C. The resultant disks were generally clear, though the FOSA copolymers exhibited a yellowish hue that increased with increasing FOSA content.

Pheniramine maleate (Sigma–Aldrich, St Louis, MO) (PM) was selected as the model drug substance for the diffusion studies. The structure for this molecule is shown in Fig. 1. This drug substance is a histamine receptor antagonist used in ocular solutions such as Visine-A<sup>®</sup> (0.3%) and, therefore, has application in the ocular drug delivery field. It is highly soluble in water and is considered to be generally stable to temperature, pH, ionic strength of the delivery medium. The molecule has a small molecular diameter (~1.4 nm), which minimizes the drug–hydrogel physical interactions as it diffuses through the polymer network, and is detectable by ultraviolet spectroscopy for assaying.

## 2.2. Drug loading

Each dried polymer disk was loaded with PM by soaking it in 10 mL of an unsaturated drug solution (18.8 mg/mL in pH 6 phosphate/acetate buffer) for 1 week. This method was preferred to in situ drug loading during polymerization to avoid any possible degradation of the drug substance or undesirable drug–polymer reaction during high temperature compression molding of the films. The wet drug-loaded polymers were vacuum dried over desiccant to remove any residual water. Because the proportion of drug in the hydrogels was significant (1–12% w/w dry), the dry polymer disks were cloudy when compared to similar disks without the drug. This degree of loading was necessary to ensure that enough drug substance was available for dissolution media assay. The equilibrium drug concentrations in the solution and in the polymer were measured in duplicate to calculate the partition

coefficient. The loading solution was assayed directly. The equilibrium drug concentration in each polymer disk was measured after exhaustive solvent extraction as has been performed in previous studies (<2% deviation after 3 days) [23].

## 2.3. Dynamic swelling

The dynamic swelling behavior was determined by soaking the dried drug loaded polymer disks in a buffered aqueous media (0.1 M phosphate–acetate buffer) at pH 4, 6, and 8 at 37 °C. This buffer range was selected because it bracketed the pH range typical of the eye and ophthalmologic solutions [24,25]. The disk mass, thickness, and diameter were measured at incremental times as the media was absorbed to monitor the dynamics of the polymer swelling.

## 2.4. Drug desorption and assay

Desorption of the PM into the media was determined using a Hanson SR8 Plus Dissolution Test Station USP type II dissolution apparatus (711) (Hanson Research, Chatsworth, CA). Each dissolution bath (37 °C) was filled with 600 mL of buffer (pH 4, 6, 8) and assumed to emulate perfect sink conditions. Samples were measured over a period of 3 days to monitor the desorption of PM from the hydrogel disk.

The concentration of PM in solution was determined using high performance liquid chromatography (HPLC) with ultra violet (UV) detection (Agilent 1100 Series, Agilent Technologies, Palo Alto, CA). The mobile phase was comprised of acetonitrile (28 vol%) and 15 mM sodium acetate (72 vol%), which was titrated to pH 5.0 with glacial acetic acid. The instrument was equipped with an Atlantis C<sub>18</sub> (3 μm), 4.6 × 150 mm<sup>2</sup> column (Waters Corporation, Milford, MA) and operated at a temperature of 23 °C, flow rate of 1.0 mL/min, 28% (v/v), detector wavelength of 265 nm, and injection volume of 10 μL. The PM retention time was approximately 4.5 min.

## 3. Results and discussion

### 3.1. Media penetration velocity and equilibrium media content

Figs. 2 and 3 show the effect of the copolymer composition and the media pH on the dynamic swelling behavior of the copolymers. As the concentration of FOSA in the copolymer increased, the rate of sorption and the equilibrium water content decreased. This is not surprising since DMA is hydrophilic and the FOSA hydrophobic, so that the equilibrium swelling capacity of the hydrogel was expected to decrease as the proportion of DMA decreased [18]. Fig. 2 shows the media sorption profiles for each of the different copolymers at pH 6 as a function of a normalized square root of time. Similar results were obtained at other pH's. The normalized time is the square root of time divided by the square of the overall disk thickness. This independent axis is used to compensate for small differences in the hydrogel disk thickness for different samples and includes the assumption that the media diffusion through the

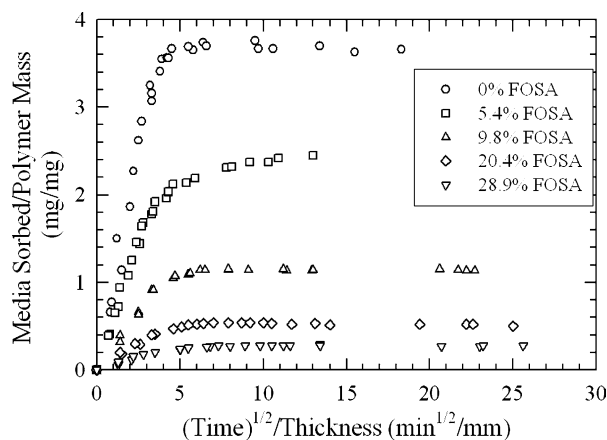


Fig. 2. Media sorption profile at pH 6 for copolymers comprised of 0–30% FOSA.

polymer was Fickian. The rate at which the glassy to rubbery front advanced from the surface to the center of the polymer disk was determined by calculating the media penetration velocity ( $v$ ),

$$v = \frac{1}{2\rho A} \frac{\partial w}{\partial t} \quad (1)$$

where  $\rho$  is the density of the media,  $A$  is the area of one disk face,  $w$  is the weight gain of the polymer and  $t$  is time. The early time data ( $t < 15$  min) where  $\partial w/\partial t$  is constant was used to calculate  $v$ . It has been suggested that as the media penetrates the glassy polymer (in these copolymers, penetration occurs presumably in the hydrophilic DMA regions), the solvent swells the polymer and creates a rubbery region [26]. Fig. 3 shows that the media penetration velocity decreased by approximately 80% and the equilibrium media content decreased by an order of magnitude as the concentration of FOSA was increased from 0 to 30 mol%. A similar degree of change in media penetration velocity was observed in hydrophobic–hydrophilic copolymers such as poly(HEMA-*co*-MMA) as the proportion of hydrophobic monomer (MMA) was increased from 0 to 40% [26,27].

The change in penetration velocity with increasing hydrophobic FOSA content may be due to two possible

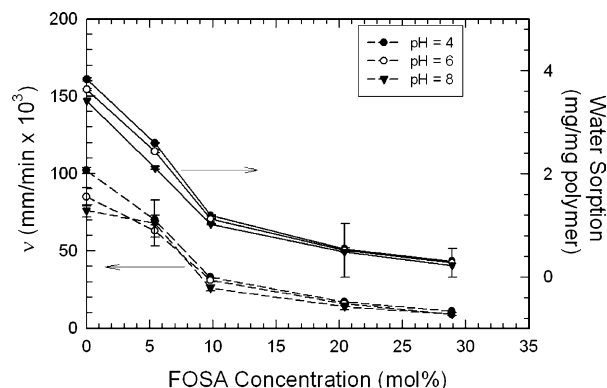


Fig. 3. Equilibrium media content at pH 4–8 in polymers comprised of 0–30% FOSA.

mechanisms. First, if the media traveled primarily through the hydrophilic DMA regions of these hydrogels, the increasing number of hydrophobic domains could obstruct the media diffusive pathway and give rise to a more tortuous pathway for diffusion. Second, the aggregated hydrophobic regions may also inhibit polymer chain relaxation, thus reducing the free volume through which the media can travel [28].

The pH of the medium appeared to have less effect on  $v$  and the equilibrium sorption, but still there was some effect, especially at the lower FOSA concentrations. In general, it appeared that  $n$  and the equilibrium sorption decreased with increasing pH. Sample DF-10 exhibited a 20% decrease in the media penetration velocity when the pH was increased from 4 to 8. Those results are consistent with the reported pH dependencies of poly(acrylamide) hydrogels [29]. At low pH, the swelling may be significantly higher due the presence of intermolecular hydrogen-bonds between adjacent carbonyl groups of the DMA that are mediated by water molecules [30]. As the solution becomes more basic, the hydrogen bonds weaken and the hydrogen-bonded structure between the chains collapses, thus inhibiting the ability of the medium to pass through the hydrogel. pH stability has been reported in copolymers comprised of poly(NIPA-*co*-FOSA) containing 2 mol% FOSA, where there was no significant change in the equilibrium swelling content between pH values of 2–12 [31]. In that case, hydrophilic acrylic acid comonomers were required to stimulate pH sensitivity, but the effect was dramatically suppressed by adding up to 5 mol% FOSA. The presence of the hydrophobic comonomer is very effective at reducing the relative pH effect for both DMA and NIPA.

The relationship between the media penetration velocity and the equilibrium media content was linear, as seen in Fig. 4, a trend that has also been observed in poly(NIPA-*co*-FOSA) copolymers [31]. Fig. 4 shows that the polymers with high media penetration velocity (i.e. permeability) also exhibited high equilibrium media content (i.e. water solubility). This suggests that the diffusivity of the water, which is related to the slope of Fig. 4 was relatively constant through the polymers (slope) since the product of the diffusivity and the solubility equals the permeability [32]. This linear relationship is also

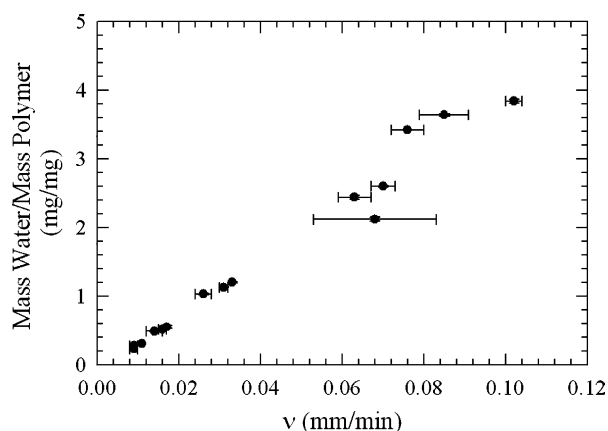


Fig. 4. Equilibrium media content at pH 4–8 as a function of media penetration velocity in the polymers comprised of 0–30% FOSA.

important because it shows that the equilibrium media content can be predicted in very short experimental time (i.e. on the order of minutes vs. days) from the media penetration velocity.

### 3.2. Change in disk thickness during swelling

Although the disk thickness increased during media sorption, see Fig. 5, the kinetics of the process were anomalous. The thickness-time profile progressed through a noticeable ‘spike’ during the early stages of swelling as evidenced by a rapid increase then decrease of the disk thickness. After the ‘spike’, the thickness gradually increased to an equilibrium state. This unexpected behavior has been previously observed for the diffusion of water in other hydrophobically modified hydrogels such as poly(HEMA-co-MMA) copolymers where a 10–20% increase followed by a ~10% decrease in initial thickness was reported [26]. In the initial stages of the media uptake, the disk’s outer edges swelled while the core remained glassy. In that state, the expansion was predominantly in the thickness direction. Once the media hydrated the glassy core, radial expansion occurred and the thickness collapsed [33], which accounts for the observed ‘spike’. Once this transition phase was complete, the disk swelled three-dimensionally to equilibrium. For the lower FOSA content copolymers, the ‘spike’ was completed in the first few minutes of swelling. However, increasing the FOSA content to 30 mol% delayed the recovery for up to ~60 min and the spike was much less dramatic, presumably due to the increased hydrophobic nature of the polymer, which slowed water influx and restricted the collapse of the glassy core. In a practical application, such as a contact lenses, hydrogels with a higher proportion of FOSA may be desirable to limit swelling and minimize the potential for undesirable in vivo movement [34].

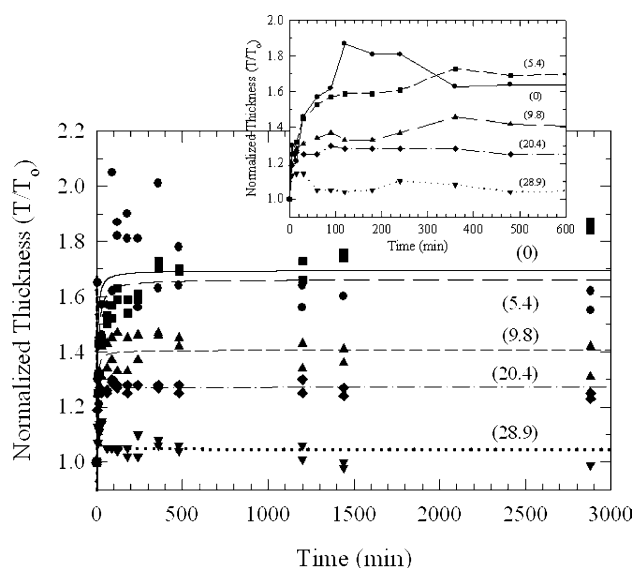


Fig. 5. Dynamic swelling hydrogel (normalized) thickness profile at pH 8 for copolymers comprised of 0–30% FOSA.

### 3.3. Media diffusion coefficients

Extensive research has been conducted to elucidate the mechanisms and models of drug release in hydrogels [35,36]. Modeling the diffusion process in hydrogels can be complicated by non-constant diffusion coefficients due to large solute loading and solvent/polymer interactions, multi-dimensional diffusion resulting in complicated solutions, changes in free volume due to solvent transport (i.e. polymer swelling/deswelling) and multi-component transport instead of single solute diffusion. These complications partially explain why no universal model has been developed that accurately describes the solute–hydrogel diffusion mechanism. The models used to describe the diffusion process in this work were based on solutions of Fick’s law,

$$\frac{\partial C}{\partial t} = D \frac{\partial^2 C}{\partial x^2} \quad (2)$$

subject to the following boundary conditions

$$t = 0, -\frac{\delta}{2} < x < \frac{\delta}{2}, c = 0; \quad t > 0, x = 0, \frac{\partial c}{\partial x} = 0;$$

$$t > 0, x = \pm \frac{\delta}{2}, c = 0$$

where  $c$  is the concentration of drug,  $t$  is time,  $x$  is position in the hydrogel,  $\delta$  is the total thickness of the hydrogel sheet, and  $D$  is the diffusion coefficient. This assumes diffusion in one dimension with constant boundary conditions [37]. The solution to this equation is an infinite series,

$$\frac{M_t}{M_\infty} = 1 - \sum_{n=0}^{\infty} \frac{8}{(2n+1)^2 \pi^2} \exp\left[\frac{-D(2n+1)^2 \pi^2 t}{\delta^2}\right] \quad (3)$$

where  $M_t$  is the mass of the hydrogel in water at  $t=t$  and  $M_\infty$  is the mass at long times when the hydrogel has reached equilibrium.

To enable reasonable modeling of the diffusion process, researchers have used three well-accepted approximations of Eq. (3): (1) the ‘early-time’ approximation (Eq. (4)) [38,39], (2) the ‘late-time’ approximation (Eq. (5)) and (3) the Eters approximation (Eq. (6)) [40]. The early-time approximation is valid for the first 60% of sorption/desorption and the late-time is valid for the latter 40%. These models were used to determine the diffusion coefficients for both media diffusion and drug diffusion. The Eters model is also used for drug diffusion as it is a semi-empirical equation derived from a statistical regression of solute diffusion profiles available in the literature and approximates the analytical solution of the entire drug release profile to within 2% error [1]. An example of the model fits is shown in Fig. 6 and is representative of the data reported in this work.

$$\frac{M_t}{M_\infty} = 4 \left[ \frac{Dt}{\pi \delta^2} \right]^{0.5} \quad (4)$$

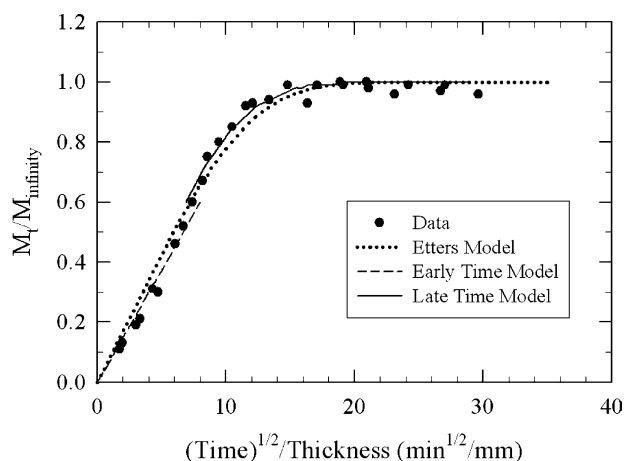


Fig. 6. Representative model fits for the early-time, late-time, and Etters approximations of Fickian diffusion through the thin disks.

$$\frac{M_t}{M_\infty} = 1 - \frac{8}{\pi^2} \exp\left[\frac{-D\pi^2 t}{\delta^2}\right] \quad (5)$$

$$\frac{M_t}{M_\infty} = \left[1 - \exp\left(-k\left(\frac{Dt}{\delta^2}\right)^a\right)\right]^{1/b} \quad (6)$$

For the Etters model,  $a$ ,  $b$ , and  $k$  were 1.3390, 2.6001, and 10.5449, respectively.

A complementary modeling method for the early-time approximation is a power law approach (Eq. (7)) [38,39], where the relative release of solute ( $M_t/M_\infty$ ) is proportional ( $k$ ) to time raised to a power ( $n$ ).

$$\frac{M_t}{M_\infty} = kt^n \quad (7)$$

The proportionality constant can be used to calculate the diffusion coefficient, and  $n$  denotes the type of transport mechanism. When  $n$  is equal to 0.5, the transport rate is Fickian (as was assumed for the early-time approximation equation)

and the drug release rate is time-dependent. When  $n$  is between 0.5 and 1.0, the drug release rate is time-dependent, but other factors such as polymer relaxation and swelling control solute transport. Case-II type diffusion occurs when  $n$  is equal to 1.0, which indicates that the release rate is time-independent. Super-case II transport occurs when  $n$  is greater than 1.0; in that case, the release rate is time-dependent.

The early-time and late-time diffusion coefficients calculated from the model fits of the sorption process are reported in Table 2. In general, there was no significant difference in the media diffusion coefficients as the proportion of FOSA was changed over the range of pH 4–8. This result agrees with the observation from Fig. 5 that the media penetration velocity was proportional to the equilibrium media content in the polymers (i.e. permeability = diffusivity  $\times$  solubility). The early-time diffusion coefficient values ranged from  $4.4 \times 10^{-3}$  to  $8.1 \times 10^{-3}$  mm<sup>2</sup>/min and the late-time diffusion coefficients ranged from  $3.9 \times 10^{-3}$  to  $7.3 \times 10^{-3}$  mm<sup>2</sup>/min. The errors in  $D$  from the fitting are also included in Table 2, and for each material, the two  $D$ 's calculated were statistically equivalent. Typical diffusion coefficient values for water diffusion in polymers are on the order of  $10^{-5}$ – $10^{-4}$  mm<sup>2</sup>/min [1], therefore, diffusion through these hydrogels is generally rapid. For comparison, the water diffusion coefficient values for poly(NIPA-*co*-Aam-*co*-HEMA) copolymers range from approximately from  $1.5 \times 10^{-4}$  to  $3.0 \times 10^{-4}$  mm<sup>2</sup>/min [41]. In these experiments there was no dramatic change in the diffusion coefficients between early and late-time for a given experimental condition, suggesting that the media diffusion rate was generally constant. This is quite interesting given that Table 2 shows that 50% of the equilibrium media mass was absorbed in less than 45 min over the range of conditions studied, while it took up to 5 h to reach 95% equilibrium.

The time values for 50 and 95% equilibrium conditions are similar to the media uptake times reported for poly(HEMA-*co*-MMA) copolymers of equivalent hydrophobic content

Table 2  
Summary of media penetration velocities, equilibrium media contents, characteristic diffusion times, media diffusion coefficients and power law parameters for the polymers

Sample	Media penetration velocity (mm/min $\times 10^3$ )	Equilibrium media sorbed (mg media/mg polymer)	$t_{0.5}^a$ (min)	$t_{0.95}^b$ (min)	$D$ , early (mm <sup>2</sup> /min $\times 10^3$ )	$D$ , late (mm <sup>2</sup> /min $\times 10^3$ )	$k$ (min <sup>-0.5</sup> )	$n$
DF0-4	102 (2)	3.84 (0.03)	32	212	6.1 (0.7)	5.3 (0.4)	0.05 (0.01)	0.57 (0.07)
DF5-4	70 (3)	2.60 (0.01)	36	289	5.4 (0.6)	3.9 (0.5)	0.07 (0.02)	0.52 (0.09)
DF10-4	33 (0)	1.20 (0.01)	45	215	4.4 (1.3)	5.3 (0.3)	0.08 (0.04)	0.63 (0.17)
DF20-4	17 (0)	0.55 (0.02)	33	182	5.9 (1.3)	6.2 (0.3)	0.11 (0.00)	0.57 (0.00)
DF29-4	11 (0)	0.31 (0.00)	36	254	5.5 (1.1)	4.4 (0.6)	0.08 (0.07)	0.57 (0.29)
DF0-6	85 (6)	3.64 (0.02)	33	178	6.0 (1.8)	6.3 (0.8)	0.07 (0.05)	0.60 (0.21)
DF5-6	63 (4)	2.44 (0.03)	32	249	6.1 (0.6)	4.5 (0.7)	0.09 (0.03)	0.44 (0.07)
DF10-6	31 (1)	1.13 (0.01)	33	178	5.9 (1.0)	6.4 (0.4)	0.13 (0.06)	0.55 (0.20)
DF20-6	16 (1)	0.52 (0.00)	29	189	6.8 (1.5)	6.0 (0.5)	0.18 (0.04)	0.41 (0.10)
DF29-6	9 (1)	0.28 (0.00)	33	193	6.0 (1.6)	5.9 (0.8)	0.14 (0.09)	0.43 (0.23)
DF0-8	76 (4)	3.42 (0.00)	32	187	6.1 (0.6)	6.0 (0.7)	0.12 (0.07)	0.46 (0.20)
DF5-8	68 (15)	2.12 (0.03)	30	206	6.5 (0.9)	5.5 (0.6)	0.08 (0.03)	0.49 (0.12)
DF10-8	26 (2)	1.03 (0.01)	45	216	4.4 (1.8)	5.2 (0.4)	0.11 (0.06)	0.55 (0.19)
DF20-8	14 (2)	0.49 (0.01)	30	186	6.4 (1.3)	6.1 (0.3)	0.17 (0.04)	0.43 (0.08)
DF29-8	9 (1)	0.23 (0.00)	24	155	8.1 (1.2)	7.3 (<0.1)	0.17 (0.06)	0.39 (0.12)

<sup>a</sup> Time required for the polymer to absorb 50% media using the early-time approximation and assuming a disk thickness of 2.0 mm.

<sup>b</sup> Time required for the polymer to absorb 95% media using the late-time approximation and assuming a disk thickness of 2.0 mm.

proportions [26]. No significant differences of the media diffusion coefficients were observed as the media pH was changed (i.e. all the data are within the 95% confidence interval). Once again, this suggests that both the poly(DMA) and its FOSA copolymers exhibit relatively stable sorption rates in environments of varying pH.

### 3.4. Media diffusion mechanism

The mode of media sorption was estimated by calculating the diffusion exponent ( $n$ ) using the power law model, Eq. (6) [39]; the values are tabulated for the different copolymers in Table 2. For the most part, over the pH range studied, the values of  $n$  for all the copolymers was close to 0.5, which indicates that the water sorption was indeed Fickian. This conclusion is consistent with the mechanism observed for water diffusion in similar hydrophilic/hydrophobic polymers, such as poly(DMA-*co-n*-butoxymethyl acrylamide) copolymers [18]. It has been proposed that the Fickian behavior is a consequence of the water molecules being much smaller than the gel network pore size. Therefore, media transport is driven by a concentration gradient rather than by convective flux [27,42]. Presumably the media is diffusing through the hydrophilic water phase in a Fickian manner and is not significantly restricted by the relaxation of the polymer.

### 3.5. Drug partitioning

Each copolymer was able to effectively absorb the drug substance into its network from a buffered media (pheniramine concentration = 18.8 g/mL). Table 3 shows that as the concentration of the hydrophobic FOSA in the copolymer increased, the equilibrium weight percent of PM decreased. Except for the sample with the highest FOSA content, DF29, the polymer-solution partition coefficients (i.e. the ratio of drug concentration in polymer to that in solution) showed that the PM exhibited a higher affinity for the polymer phase. The preference for the polymer phase, though, did decrease with increasing FOSA concentration. Partition coefficients slightly above unity have also been observed for hydrophilic solutes such as Orange II in poly(acrylamide) hydrogels [43]. Since, the water molecules form hydrogen bonds with the polymer matrix, the drug may associate somewhat more closely in the polymer phase.

Table 3  
Equilibrium drug loading conditions for PM in each polymer

Sample	Volume swollen polymer/mass dry polymer ( $\text{cm}^3/\text{mg} \times 10^3$ )	Equilibrium PM concentration in dry polymer (wt%)	Equilibrium PM concentration in swollen polymer ( $\text{mg}/\text{cm}^3$ )	Partition coefficient
DF0	4.5 (0.1)	11.6 (0.3)	25.8 (0.5)	1.4
DF5	3.2 (0.1)	9.9 (0.2)	31.3 (0.7)	1.7
DF10	1.9 (0.0)	6.4 (0.1)	34.0 (0.7)	1.8
DF20	1.2 (0.0)	2.7 (0.0)	23.1 (0.3)	1.2
DF29	1.0 (0.0)	1.3 (0.0)	13.0 (0.0)	0.7

It is not surprising that the drug preferentially partitioned into the more hydrophilic polymer. This phenomenon could be due to the phase structure of the copolymers. It has been shown that within the polymer, the strong and reversible associations between the FOSA perfluoro side chains form hydrophobic domains that are surrounded by a hydrophilic matrix [6]. Microphase separation is caused by polymer–polymer (i.e. DMA–FOSA) incompatibility of the hydrophobic perfluoro groups, which possess relatively low cohesive energy density and surface energy [31], with the hydrophilic DMA. The hydrophobic associations of the fluorocarbon groups are stronger than their hydrocarbon counterparts because the fluorinated  $\text{CF}_2$  groups are 1.7 times more hydrophobic than  $\text{CH}_2$  groups. The microstructure of these copolymers has recently been characterized and shown to be comprised of polydisperse spherical FOSA nanodomains surrounded by a water-poor shell of DMA, all of which is surrounded by a water-swollen DMA matrix [21]. Presumably the highly soluble drug molecule resides primarily in the hydrophilic water-rich DMA phase as previously proposed for core–shell models and hydrophilic drugs [44]. It is unlikely that any drug is absorbed into the water-poor hydrophobic FOSA regions because initial swelling experiments demonstrated that water was not absorbed by the homopolymer poly(FOSA).

### 3.6. Drug diffusion: overall release of PM

The rate of drug release was determined by measuring the concentration of PM in the surrounding dissolution media as the drug diffused from the polymers. A representative drug release profile is shown in Fig. 7, where the fractional release of the drug from the polymer is plotted against the normalized square root of time. These data show that the overall drug release rate from the polymers decreased as the FOSA composition of the copolymers increased. As reported previously for the solvent penetration and subsequent release of thiamine–HCl in poly(HEMA) hydrogels, it is likely that the osmotic pressure formed by the highly water soluble drug, the swelling force of the hydrophilic DMA phase and

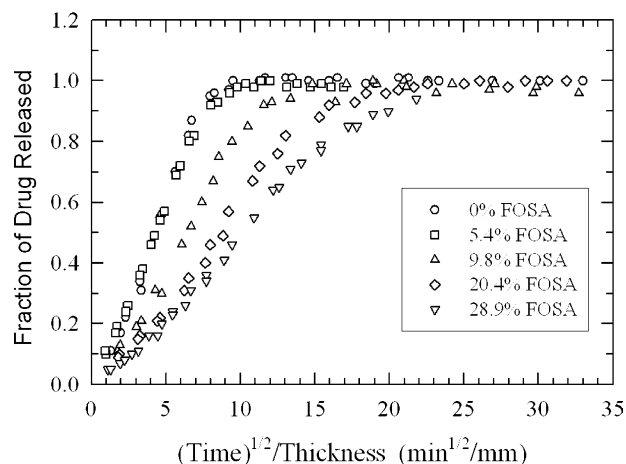


Fig. 7. Drug release profile of PM from the 30% FOSA copolymer at different pH.

Table 4  
Summary of the characteristic drug diffusion times, drug diffusion coefficients, power-law parameters and swelling interface numbers

Sample	$t_{0.5}^a$ (min)	$t_{0.95}^b$ (min)	$D$ , early ( $\text{mm}^2/\text{min} \times 10^3$ )	$D$ , late ( $\text{mm}^2/\text{min} \times 10^3$ )	$D$ , Etters ( $\text{mm}^2/\text{min} \times 10^3$ )	$k$ ( $\text{min}^{-0.5} \times 10^2$ )	$n$	$Sw$ ( $t=0$ ) <sup>c</sup> , ( $t=\infty$ ) <sup>d</sup>
DF0-4	64	258	3.08 (<0.01)	4.38 (0.44)	3.92 (<0.01)	4.3 (0.0)	0.58 (0.02)	33, 35
DF5-4	65	291	3.01 (0.16)	3.88 (0.25)	3.54 (<0.01)	4.2 (1.1)	0.54 (0.06)	23, 27
DF10-4	171	619	1.15 (0.09)	1.82 (0.13)	1.60 (0.12)	5.4 (1.5)	0.54 (0.08)	29, 27
DF20-4	259	1226	0.76 (0.08)	0.92 (0.04)	0.92 (0.08)	3.6 (0.7)	0.58 (0.05)	23, 28
DF29-4	346	1640	0.57 (0.05)	0.69 (0.08)	0.71 (0.06)	1.9 (0.9)	0.57 (0.09)	20, 24
DF0-6	85	301	2.32 (0.42)	3.75 (0.39)	3.14 (0.37)	6.6 (0.1)	0.53 (0.02)	37, 34
DF5-6	78	348	2.51 (<0.01)	3.24 (0.16)	2.93 (<0.01)	4.0 (0.6)	0.55 (0.04)	25, 29
DF10-6	181	747	1.09 (0.14)	1.51 (0.11)	1.36 (<0.01)	4.1 (1.1)	0.60 (0.07)	29, 31
DF20-6	333	1593	0.59 (0.06)	0.71 (0.07)	0.73 (0.06)	2.9 (1.1)	0.60 (0.08)	27, 33
DF29-6	465	2026	0.42 (0.03)	0.56 (0.01)	0.51 (0.03)	1.5 (0.4)	0.59 (0.05)	22, 25
DF0-8	109	355	1.81 (0.59)	3.18 (0.27)	2.65 (0.37)	6.4 (0.0)	0.50 (0.00)	42, 36
DF5-8	82	393	2.40 (0.20)	2.87 (0.23)	2.67 (0.19)	3.3 (1.0)	0.57 (0.07)	29, 36
DF10-8	180	927	1.09 (0.07)	1.22 (0.11)	1.17 (0.08)	4.6 (0.4)	0.55 (0.02)	24, 32
DF20-8	456	1632	0.43 (0.04)	0.69 (0.08)	0.51 (0.04)	2.5 (0.8)	0.60 (0.07)	34, 31
DF29-8	521	2429	0.38 (0.04)	0.47 (0.02)	0.43 (0.03)	1.2 (0.4)	0.61 (0.06)	23, 28

<sup>a</sup> Time required for the diffusion of 50% drug using the early-time approximation and a disk thickness of 2.0 mm.

<sup>b</sup> Time required for the diffusion of 95% media using the late-time approximation and a disk thickness of 2.0 mm.

<sup>c</sup> Swelling interface number at time equal to zero assuming an initial disk thickness of 2.0 mm.

<sup>d</sup> Swelling interface number at time equal to infinity (equilibrium) assuming an equilibrium disk thickness of 2.0 mm.

the contraction of the hydrophobic FOSA phase contribute to the changes in the drug release rate [45]. Table 4 shows the time required for 50 and 95% release of the drug substance for each copolymer and pH condition. By increasing the FOSA content from 0 to 30 mol%, the time required for 50% release increased from about 1 to nearly 8 h. That effect was even more prominent at the 95% release condition where the amount of drug released was extended from 4 h to nearly 1.5 days for the DF0 and DF29 samples, respectively. These findings are consistent with desorption of FTIC-insulin from other hydrophobic–hydrophilic copolymers, such as poly(NIPA-*co*-sodium acrylate-*co*-*n*-N-acrylamide), where clustering of the long alkyl chain lengths created similar hydrophobic micro-regions, which decreased the quantity of drug released for a given time [23].

The media pH also had a significant affect on the overall drug release profile. As pH was increased, the amount of drug released at any given time was lower. Fig. 8 shows example dissolution profiles for the DF29 copolymer at pH's of 4, 6 and 8. The time required for 95% drug release in the DF29 copolymers nearly doubled from 27 to 41 h for pH 4 and 8, respectively (Table 4). This is consistent with the equilibrium media sorption data reported earlier in this paper, where the media sorption decreased (i.e. deswelling occurred) with increasing pH. For DF29, there was 26% less aqueous media in the polymer at pH 8 than at pH 4. Therefore, the swollen hydrophilic regions through which the drug can diffuse would be smaller and/or closer in proximity. It is unlikely that the solubility of the PM greatly affected the dissolution rate since the drug substance is highly soluble in aqueous solution and the  $pK_a$  of the drug substance was 8.8. This suggests that the drug almost instantaneously dissolved into the penetrating media and the pH and hydrophobic content were the primary contributors to the drug release behavior.

### 3.7. Drug diffusion: modeling the diffusion process and determination of the diffusion coefficients

The diffusion coefficients for each copolymer and media condition were determined using the early-time approximation (Eq. (4)), late-time approximation (Eq. (5)), and Etters approximation (Eq. (6)) [40]. An example of the model fits for a representative data set is shown in Fig. 6. These three models were determined to be acceptable for these data as the mean variance values (as determined from the 95% confidence intervals) for the diffusion coefficients were 10, 8, and 6%, respectively. A small but noticeable trend in the values of the diffusion coefficients was observed among the different diffusion models for a given condition. In general, the rank order of diffusion coefficients was late-time > Etters > early-time, where the late-time approximation was  $36 \pm 19\%$  higher than the early-time diffusion coefficient. It seemed that the

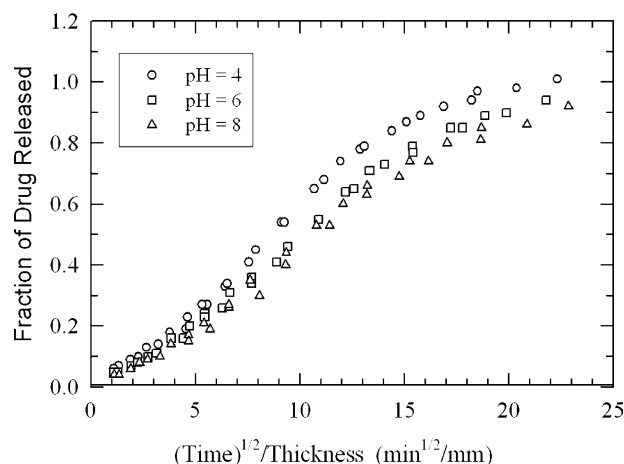


Fig. 8. Drug diffusion coefficients (Etters approximation) for polymers in different media pH.



solution proposed by Etters ‘smoothed’ the transition in the profile between the early and late diffusion times. As expected, the diffusion coefficient was higher when the hydrogel was in its more hydrated form (i.e. at later times) and the drug substance could diffuse more quickly through the increased volume of the hydrophilic phase.

For the copolymers studied, the early-time diffusion coefficients, late-time diffusion coefficients, and Etters diffusion coefficients ranged from  $0.4 \times 10^{-3}$  to  $3.1 \times 10^{-3}$ ,  $0.5 \times 10^{-3}$  to  $4.4 \times 10^{-3}$ , and  $0.4 \times 10^{-3}$  to  $3.9 \times 10^{-3}$  mm<sup>2</sup>/min, respectively, see Table 4 and Fig. 9. The effect of the FOSA concentration on the diffusion constant is shown for the Etters model in Fig. 9; the other models show similar trends. As the hydrophobicity of the polymers increased (e.g. increasing FOSA content), the diffusion coefficient decreased significantly. For example, the diffusion coefficient (early-time) for the poly(DMA) polymer was five times greater than the diffusion coefficient for the D29-6. Although not as dramatic as changing FOSA content, a change in media pH had a measurable effect on the drug diffusion coefficient. As the media pH was increased, the diffusion coefficient for the polymer decreased. For example, the late-time diffusion coefficients for any given poly(DMA-co-FOSA) copolymers decreased by about 30% as the pH of the media was increased from 4 to 8. These data suggest that FOSA content can be used to ‘coarsely’ tune drug release behavior (>2X) and pH could be used to ‘finely’ tune drug release behavior (<2X) over the range of conditions studied in these experiments.

### 3.8. Comparison of drug transport rate in the polymers and bulk solution

The drug substance diffusion coefficients in the copolymers were compared to the theoretical diffusivity of the drug substance at infinite dilution to assess the validity of the experimentally determined diffusion coefficients. The diffusion coefficients in the copolymers should be lower than the diffusion coefficients at infinite dilution due to hindrances from the polymer network. The diffusivity of a solute at infinite

dilution can be predicted from the methods developed by Stokes–Einstein (Eq. (8)) or Hayduk–Laudie (Eq. (9)) [46].

$$D_{\infty} = \frac{kT}{6\pi\mu r} \quad (8)$$

$$D_{\infty} = \frac{8.621 \times 10^{-14}}{\mu^{1.14} V^{0.589}} \quad (9)$$

where  $D_{\infty}$  = diffusivity of PM in water (m<sup>2</sup>/s),  $k$  = Boltzmann constant ( $1.38065 \times 10^{-23}$  m<sup>2</sup> kg s<sup>-1</sup> K<sup>-1</sup>),  $T$  = absolute temperature, 310 K,  $\mu$  = viscosity of water at 310 K,  $0.6950 \times 10^{-3}$  Pa s,  $r$  = equivalent spherical radius of PM,  $6.8435 \times 10^{-10}$  m, and  $V$  = molar volume of PM,  $0.2945$  m<sup>3</sup>/kmol.

The Stokes–Einstein equation describes the movement of a ‘hard’ sphere through a viscous liquid, where the liquid at the sphere surface is moving at the same velocity as the sphere. This relation describes the frictional resistance of the sphere as it travels through the liquid, which is inversely proportional to the diffusion rate of the sphere. As the friction between the moving molecule and the liquid increases, the diffusion coefficient decreases. The equivalent spherical radius of PM in water (eight molecules in a unit cell, each with a radius of 6.84 Å) was determined from X-ray diffraction data [47]. The Hayduk–Laudie equation was developed for measuring the diffusion coefficients of non-electrolytes in dilute aqueous solutions, and it has been shown to approximate diffusion coefficients with less than 20% relative error [48].

The Stokes–Einstein diffusivity of PM and the Hayduk–Laudie diffusivity were  $28.7 \times 10^{-3}$  and  $42.3 \times 10^{-3}$  mm<sup>2</sup>/min, respectively. The diffusivity value from the Hayduk–Laudie equation was probably high since it was determined using the PM molar volume at room temperature instead of at the model-prescribed normal boiling point of PM. One might expect the molar volume to be higher at the normal boiling point ( $\gg 310$  K), and thus the diffusivity value somewhat lower. In any case, the two equations gave similar values and, therefore, were considered to be generally acceptable for comparison to the experimental data.

As expected, the diffusion coefficients determined from the dissolution experiments ( $0.4 \times 10^{-3}$ – $4.4 \times 10^{-3}$  mm<sup>2</sup>/min) were much lower than the values calculated from the Stokes–Einstein and Hayduk–Laudie equations. Presumably, the hydrophobic regions in the polymers inhibited the diffusive pathway, thereby slowing the diffusion of the drug through the hydrophilic DMA regions. Assuming that the Stokes–Einstein diffusivity value was representative, the diffusion rate can, in principle, be decreased from approximately 6–70 times by selecting the appropriate combination of media pH and FOSA content of the copolymer. This is an exciting discovery because it shows that drug delivery systems based on these polymers should be better for controlling drug substance dosage than standard liquid dosage forms (e.g. in eye drop solutions) currently used.

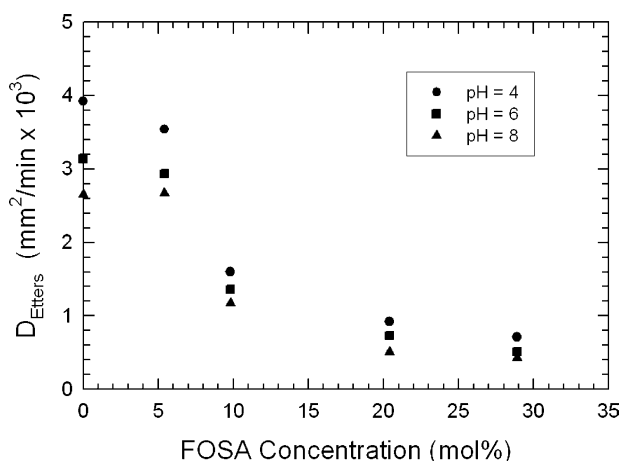


Fig. 9. Drug diffusion coefficients (Etters approximation) for copolymers in different media pH.

### 3.9. Drug release mechanism

The mass transport mechanism for drug diffusion through the polymer was evaluated to determine if the diffusion rate was controlled by Fickian type diffusion, swelling of the polymer or, perhaps, both. The 95% drug release time was an order of magnitude greater than the time required to achieve 95% media sorption equilibrium (cf. Tables 2 and 4), especially for the polymers comprised of higher concentrations of FOSA. This indicates that the media diffused through the polymer much faster than the drug substance. Presumably the drug dissolved immediately inside the polymer disk as soon as it contacted the water because in this system the drug was significantly below its aqueous solubility limit ( $\sim 50 \text{ mg/cm}^3$ ). Once hydrated, the densely packed polymer chains, physical crosslinks, and hydrophobic nanodomains most likely restricted the diffusion of the drug through the polymer network. Based on these data alone, the mass transport kinetics are diffusion rate controlled rather than swelling rate controlled.

The drug mass transport mechanism was evaluated by calculating the diffusion exponent ( $n$ ) of the power law model, Eq. (7), and the calculations are summarized in Table 4. The values of  $n$  were between 0.5 and 0.6. Overlap of the 95% confidence intervals suggested no significant differences in the value of  $n$  as a function of pH or FOSA content.

The swelling interface number ( $Sw$ ) (Eq. (10)) was also used to determine the type of drug transport mechanism [49].  $Sw$  describes the relationship between the convective velocity of water ( $v$ ) and drug diffusivity ( $D$ ) as a function of gel layer thickness ( $\delta$ ) and time ( $t$ ). When  $Sw$  values are approximately equal to one, solute release is both swelling-dependent and diffusion-dependent. Hydrogels that exhibit  $Sw$  values much greater than unity demonstrate Fickian behavior where the drug diffusion rate is controlled by the mass transport rate.

$$Sw = \frac{v\delta(t)}{D} \quad (10)$$

The swelling interface numbers given in Table 4 also indicated that the diffusion mechanism was significantly diffusion controlled, i.e. the  $Sw$  values were much greater than unity. Brazel and Peppas [27] reported that values of  $Sw$  were consistently around unity when values of the power-law exponent ( $n$ ) were above 0.7. Typically, when  $Sw$  values were  $\gg 1$ , the power-law exponent was approximately 0.5. Although it has been suggested that the values of  $n$  and  $Sw$  may not comprehensively describe the diffusion process [50], it is apparent that these values provide a useful explanation for how diffusion controls the drug release mechanism in these hydrophobic–hydrophilic copolymers.

## 4. Conclusions

The physically crosslinked hydrogel copolymer comprised of a hydrophilic monomer (DMA) and a hydrophobic monomer (FOSA) has proven to be effective in controlling the desorption rate of a drug substance from its matrix. Copolymerizing the

FOSA with the DMA-based hydrogels decreased (1) the media penetration velocity through the hydrogels, (2) the change in hydrogel volume during swelling, (3) the equilibrium media content in the hydrogels, (4) and the drug diffusion rate through the hydrogels. The pH of the aqueous media into which the drug substance diffused had a much less dramatic effect on the hydrogel, but nevertheless increasing the media pH slightly slowed the diffusion of the drug substance by decreasing the swellability of the hydrogel. This is a desirable attribute for a hydrogel when subjected to environments of varying pH because it is relatively stable (does not exhibit a volume phase transition). Diffusion models fitted to the experimental data showed that the drug diffusion rates through the copolymers were primarily Fickian, as shown by the values of the diffusion exponent ( $n \approx 0.5$ ), and the swelling interface numbers ( $Sw \gg 1$ ). This indicated that the drug desorption was controlled by diffusion rather than by hydrogel swelling. The ability of these novel copolymers to deliver a drug substance at a controlled rate suggests that these hydrogels show great promise as a drug delivery system.

## Acknowledgements

The authors thank Dr Jun Tian for participating in stimulating research discussions and contributing his technical expertise. Pfizer Global Research and Development is acknowledged for providing laboratory facilities to conduct these experiments. Partial support of this work was provided by the Petroleum Research Fund of the American Chemical Society, Grant No. 36649-AC7.

## References

- [1] Korsmeyer RW. In: Tarcha PJ, editor. *Polymers for controlled drug delivery*. Boca Raton: CRC Press; 1991. p. 16–34.
- [2] Yamada-Nosaka A, Ishikiriyama K, Todoki M, Tanzawa HJ. *Appl Polym Sci* 1990;39:2443–52.
- [3] Ferreira L, Vidal MM, Gil MH. *Chem Educator* 2001;6:100–3.
- [4] Hoffman AS. *Adv Drug Deliv Rev* 2002;43:3–12.
- [5] Blanco MD, Gomez C, Garcia O, Teijon JM. *Polym Gels Networks* 1998; 6:57–69.
- [6] Bae SS, Chakrabarty K, Seery TAP, Weiss RA. *J Macromol Sci, Pure Appl Chem* 1999;A36:931–48.
- [7] Muratore LM, Davis TP. *J Polym Sci, Part A: Polym Chem* 2000;38: 810–7.
- [8] Kunzler J, Ozark R. *J Appl Polym Sci* 1997;65:1081–9.
- [9] Lai Y-C, Valint PL. *Polym Mater Sci Eng* 1995;72:116–7.
- [10] Lai Y-C, Valint PL, Friends G. *Polym Mater Sci Eng* 1997;76:34–5.
- [11] Amis EJ, Hu N, Seery TAP, Hogen-Esch TE, Yassini M, Hwang F. Hydrophilic polymers: performance with environmental acceptance. In: Glass JE, editor. *Advances in chemistry series*, vol. 248. Washington, DC: American Chemical Society; 1996. p. 279–302.
- [12] Da J, Hogen-Esch TE. *Macromolecules* 2003;36:9559–63.
- [13] Seery TAP, Yassini M, Hogen-Esch TE, Amis EJ. *Macromolecules* 1992; 25:4784–91.
- [14] Tomczak S, Hogen-Esch TE. *Polym Prepr* 2001;42:562–3.
- [15] Tomczak S, Hogen-Esch TE. *Polym Prepr* 2003;44:1175–6.
- [16] Bae YH, Okano T, Ebert C, Heiber S, Dave S, Kim SW. *J Controlled Release* 1991;16:189–96.
- [17] Delgado M, Spanka C, Kerwin LD, Paul Wentworth J, Janda KD. *Biomacromolecules* 2002;3:262–71.

- [18] Lee WF, Yeh PL. *J Appl Polym Sci* 1997;65:909–16.
- [19] Meerwall EV, Cregger T, Shamlou S, Kennedy JP. *Polym Prepr* 1997;38: 869–70.
- [20] Tian J, Seery TAP, Ho DL, Weiss RA. *Macromolecules* 2004;37: 10001–8.
- [21] Tian J, Seery TAP, Ho DL, Weiss RA. *Polym Mater Sci Eng* 2003;89: 714–5.
- [22] Tian J, Seery TAP, Weiss RA. *Macromolecules* 2004;37:9994–10000.
- [23] Yu H, Grainger DW. *J Controlled Release* 1995;34:117–27.
- [24] Physicians' Desk Reference. Thompson Micromedex; 2004.
- [25] Yamada M, Mochizuki H, Kawai M, Yoshino M, Mashima Y. *Curr Eye Res* 1997;16:482–6.
- [26] Davidson R, Peppas NA. *J Controlled Release* 1986;3:243–58.
- [27] Brazel CS, Peppas NA. *Biomaterials* 1999;20:721–32.
- [28] Chen LLH. *Pharm Dev Technol* 1998;3:241–9.
- [29] Ramaraj B, Radhakrishnan G. *J Appl Polym Sci* 1994;52:837–46.
- [30] Hajime M, Ishida K, Tamaki E, Satoh M. *Polymer* 2002;43:103–10.
- [31] Tian Q, Zhao Z, Tang X, Zhang Y. *J Appl Polym Sci* 2003;87: 2406–13.
- [32] Geankoplis CJ. *Transport processes and unit operations*. 3rd ed. Englewood Cliffs, NJ: Prentice Hall; 1993.
- [33] Ji S, Ding J. *Polym J* 2002;34:267–70.
- [34] Sanzgiri YD, Maschi S, Crescenzi V, Callegaro L, Topp EM, Stella VJ. *Proc Int Symp Control Rel Bioact Mater* 1993;20:382–3.
- [35] Narasimhan B, Peppas NA. *Controlled drug delivery*. In: Park K, editor. ACS symposium series, vol. 752. Washington, DC: American Chemical Society; 1997. p. 529–57.
- [36] Amsden B. *Macromolecules* 1998;31:8382–95.
- [37] Crank J. *The mathematics of diffusion*. 2nd ed. Oxford: Oxford University Press; 1975.
- [38] Ritger PL, Peppas NA. *J Controlled Release* 1987;5:37–42.
- [39] Ritger PL, Peppas NA. *J Controlled Release* 1987;5:23–36.
- [40] Eppers JN. *Text Chem Color* 1980;12:140–5.
- [41] Lee WF, Shieh CH. *J Appl Polym Sci* 1999;71:221–31.
- [42] Gehrke SH, Vaid N, Uhden L. *Proc Int Symp Control Rel Bioact Mater* 1995;22:145–6.
- [43] Guilherme MR, Silva R, Giroto EM, Rubira AF, Muniz EC. *Polym Gels Networks* 2003;22:4213–9.
- [44] Kim YJ, Kim SW. *Polymer gels*. In: Bohidar HH, editor. ACS symposium series, vol. 833. Washington, DC: American Chemical Society; 2003. p. 300–11.
- [45] Lee PIJ. *J Controlled Release* 1985;2:277–88.
- [46] Hayduk W, Laudie H. *AIChE J* 1974;20:611–5.
- [47] Parvez M, Rusiewicz M. *Acta Crystallogr Sect C: Cryst Struct Commun* 1996;C52:83–5.
- [48] Li J, Carr PW. *Anal Chem* 1997;69:2530–6.
- [49] Peppas NA, Franson NM. *J Polym Sci, Polym Phys Ed* 1983;21:983–97.
- [50] Soppirath KS, Amanabhavi TM. *J Eur Pharm Biopharm* 2002;53:87–98.